



Original paper

Predicting the discharge coefficient of triangular plan form weirs using radian basis function and M5' methods

Azam Akhbari¹, Amir Hossein Zaji^{2,*}, Hamed Azimi², Mohsen Vafaeifard¹¹Department of Civil Engineering, Faculty of Engineering, University of Malaya, Kuala Lumpur, Malaysia.²Young Researches Club, Kermanshah Islamic Azad University.

ARTICLE INFO

Article history:

Received 30 December 2017

Received in revised form 20 January 2017

Accepted 3 February 2017

Keywords:

Triangular plan form weir
Discharge coefficient
Radial basis neural networks
M5' method
Sensitivity analysis

ABSTRACT

Weirs are installed on open channels to adjust and measure the flow. Also, discharge coefficient is considered as the most important hydraulic parameter of a weir. In this study, using the Radial Base Neural Networks (RBNN) and M5' methods, the discharge coefficient of triangular plan form weirs is modeled. At first, the effective parameters in the prediction of the discharge coefficient are identified. Then, by combining the input parameters, for each of the RBNN and M5' methods, six different models are introduced. By analyzing the modeling results for all models, it was shown that the M5' model is capable of modeling the discharge coefficient more accurately. Also, based on the modeling results, a model that considered the impact of all input parameters was introduced as a superior model. The mean absolute percentage error (MAPE) and correlation coefficients (R^2) values for the preferred model in the test mode were calculated 2.774 and 0.831, respectively. Also, for each of the M5' models, some relationships were proposed to estimate the triangular plan form weirs. The evaluation of these relationships showed that the parameters of the ratio of head over the weir to channel width (h/B) and Froude number (Fr) were the most effective parameters in the prediction of the discharge coefficient.

© 2017 Razi University-All rights reserved.

1. Introduction

The weirs with various shapes are installed as a barrier, orthogonal to the flow direction, to measure and regulate the water within the open channels. Weirs typically are used as rectangular, triangular, circular, composite, sinusoidal and labyrinth shapes in irrigation channels, drainage networks, and other hydraulic targets.

Many researchers have conducted laboratory, analytical and theoretical studies on the hydraulic behavior of normal weirs. Schoder and Turner (1929) proposed an equation to calculate the discharge coefficient of a steep-rectangular weir. The discharge coefficient was presented as a function of flow head over weir crest to weir height. The discharge coefficient of the proposed equation is considered without the effects of viscous and capillary effects. Rouse (1936) also presented a discharge coefficient equation for normal weirs in the case of the ratio of head over weir to the weir height are greater than 15. Kandaswamy and Rouse (1957), using the results of a laboratory study, obtained a solution to calculate the discharge through normal weirs. Strelkoff (1964) estimated the discharge coefficient of this type of hydraulic structures for a condition that the ratio of head over weir to weir height is less than ten by assuming a two-dimensional flow through a sharp weir edges using the analytical method. Taylor (1968) examined the hydraulic behavior of the labyrinth weirs. Hay and Taylor (1969) studied the different states of labyrinth weirs. The results showed that the placement panels as the triangular shape is more efficient than the labyrinth state. Hager (1983) conducted a study to calculate the discharge coefficient of normal weirs by using the geometric specification of the channel and the depth of the brink depth. Ramamurthy, Tim et al. (1987) estimated the discharge coefficient of a sharp-crested weir using the Momentum principles. Swamee (1988) obtained an equation to calculate the discharge coefficient of normal rectangular weirs. The Swamee's equation was a function of the geometric specification of the weir and the flow head over normal weir. Tullis et al. (1995) from the trapezoidal labyrinth weirs found that the discharge capacity of this type of weirs is a function of the total head on

the weir, the effective crest length of the weir and the discharge coefficient of the weir. Wormleaton and Soufiani (1998) conducted a laboratory study concerning the hydraulic specification and aerodynamic of triangular labyrinth weir. It was found that the aeration efficiency of triangular labyrinth weir is higher than the linear weirs with more equal length. Johnson (2000) proposed a relationship to calculate discharge coefficient of the rectangular weirs in the flat-topped and sharp-crested. Emiroglu and Baylar (2006) examined the effects of the included angle and sill slope of the weir on triangular labyrinth weir aeration. Tullis, Young et al. (2007) investigated the effects of submergence on the hydraulic behavior of labyrinth weir in and obtained a relationship between the discharge through the crest and the normal weir head. Bagheri and Heidarpour (2010) obtained an equation to calculate the discharge coefficient of the normal rectangular weir using a laboratory study. The discharge coefficient equation is a function of the ratio of the width of the weir to the channel width and the ratio of the weir head to weir height. Kumar, Ahmad et al. (2011) determined the by discharge capacity of a triangular planform weirs. Ahmad et al. (2011) are considered discharge coefficient of Kumar as a function of geometric weir characteristics and hydraulic parameters of flow.

In recent decades, soft computing and artificial intelligence have been used in the prediction and modeling of nonlinear phenomena by researchers from various sciences. Also, different artificial neural network algorithms have been widely used to solve multiple problems of hydraulic science, hydrology and water resources. Savi et al. (1999) modeled and predicted the runoff of the rainfall. Giustolisi (2004) calculated the resistance coefficient of the corrugated channels using the neural network algorithm GP. Bilhan et al. (2010) predicted the discharge coefficient of the sharp-crested rectangular weir on the wall of a straight channel using various neural network techniques such as Feed Forward Neural Networks (FFNN) and Radial Basis Neural Networks (RBNN). Dursun et al. (2012), using the ANFIS model, presented a relationship to calculate the discharge coefficient of semi-elliptical side weirs over the side of the rectangular channels in sub-

*Corresponding author Email: amirzaji@gmail.com

critical flow conditions. Also, Kisi Emiroglu et al. (2012) modeled the discharge of the labyrinth triangular weir located on a rectangular channel using radial base neural networks (RBNN), generalized regression neural networks (GRNN) and gene expression programming (GEP). They obtained an equation as a function of the upstream weir of Froude number and the geometric characteristics of the weir and the main channel. Azamathulla and Ahmad (2013) predicted the discharge through a rectangular slide gate on open channels, using the gene expression programming algorithm. They proposed a relationship as a function of the flow Froude number and the ratio of the flow depth at the upstream gate to the gate opening to calculate the discharge coefficient of this type of structures. Ebtehaj et al. (2015) predicted the discharge coefficient of rectangular side orifices on the wall of rectangular channels in sub-critical conditions by the GMDH neural network model.

From the literature, it should be noted that the study of the triangular plan form weirs requires further investigation. On the other hand, the use of various artificial intelligence techniques for modeling the drainage capacity of these structures is considered as an optimal and appropriate solution that contains important and practical points. Therefore, in this study, the discharge capacity of the triangular plan form weirs which are installed in the rectangular channels is modeled using Radial Base Neural Networks (RBNN), and Method modified M5 (M5'), and the results of these two methods are compared with each other. For this purpose, the effective parameters are determined by the discharge coefficient firstly. Subsequently, by combining the input parameters, for each of the RBNN and M5' methods, six different models are introduced. Then, by analyzing the results of the modeling, the superior models to predict the discharge coefficient of the triangular plan form weirs are introduced.

2. Experimental Model

In this study, for the verification of the results of RBNN and M5' methods, Kumar et al. (2011) laboratory measurements are used. A laboratory model of Kumar et al. (2011) includes a rectangular channel with a length of 12 meters, a width of 0.28 meters and a depth of 0.41 meters. The triangular planform weir is made of steel plates, which is located in a rectangular entrance channel 11 meters. A pipe provides the input flow into the rectangular channel through a fixed-headed air reservoir. A point gage measures the head of the triangular weir crest with an accuracy. To aerate the nappe over the weir, the aeration holes are embedded on the sides of the lateral walls of the rectangular channel. In the upstream of the rectangular channel, grid walls and wave suppressors are used to reduce disturbances and eddies. In the laboratory model and are the included-angle of the weir, the height of weir, the head of the flow over the weir and the discharge flow over the weir, respectively. In Table 1, the range of laboratory measurements of Kumar et al. (2011) study is shown. Also in Fig. 1, the general scheme of the laboratory model of Kumar et al. (2011) has been depicted.

Table 1. The range of laboratory values of Kumar et al. (2011).

θ	w	H	Q
30	0.0924	0.0079–0.0346	0.0020–0.0125
60	0.1005	0.0129–0.0565	0.0021–0.0120
90	0.1029	0.0136–0.0689	0.0015–0.0121
120	0.1062	0.0197–0.0725	0.0021–0.0124
150	0.1075	0.0142–0.0710	0.0012–0.0113
180	0.1000	0.0242–0.0724	0.0022–0.0109

3. Numerical methods

3.1. M5' model tree

The decision tree is a sequence of tests that determine the appropriate test at each step. A decision tree is a tree in which branch nodes represent a choice between alternatives, and leaf nodes represent a decision of the desired class. Generally, in a decision tree, data begins to be divided by the root, and eventually, in the leaf nodes are divided into different classes. In each node, the values of a sample are tested, and then, according to some of the attributes of that sample, one of the branches of that node is selected and also move downward (Hand. 2007; Kantardzic. 2011). As it is clear, in decision trees, the response variable is a label. But to solve the problems in which target variables are numerical, regression trees presented by Breiman,

Friedman, et al. (1984) is used. It should be noted that regression trees and decision trees are not structurally different from each other, and the only difference is how to deal with target variables. The model trees introduced by Quinlan (1992) is an extension of regression trees in which each leaf is a multivariable linear regression model. In fact, model trees are a decision tree that is modeled for a continuous class problem. Also, instead of class names, at each leaf, a line is fitted on each class. M5 model tree was presented for the first time by Quinlan (1992) and then examined and improved by Wang and Witten (1996) as M5'. Similar to the situation that occurred in the decision tree, in M5' the dataset space is divided into several parts and in the first step a regression tree is constructed.

The M5' divides the primal dataset by using the Standard Deviation (SD) of the classes' members and tries to decrease this error by testing all of the attributes of that node. The Standard Deviation Reduction (SDR) is defined as follow:

$$SDR = sd(T) - \sum \frac{|T_i|}{|T|} SD(T_i) \tag{1}$$

where T is the samples that reach to a specified node, and i is the number of the outcome of the potential set. After the tree is formed, the M5' based on the samples in each decision node and leaf node develops a linear regression for that node. Then the leaves of the tree that estimate target values with low accuracy will be pruned, and the final shape of the model is obtained.

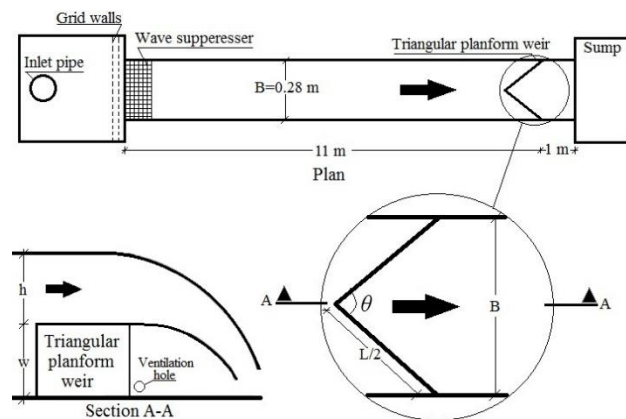


Fig. 1. The general scheme of the laboratory model of Kumar, Ahmad et al. (2011).

3.2. Radial basis neural network

The training algorithm of RBNN (Broomhead and Lowe 1988; Moody and Darken 1989; Poggio and Girosi 1990) is mostly faster than the back propagation neural networks and the probability of trapping in the local minimum is lower (Kisi et al. 2008; Ay and Kisi 2011). So that, this method is very appropriate for the complex hydraulic engineering problems. RBNN is a supervised learning algorithm that forms from three layers namely the input layer, the hidden layer, and the output layer. The input variables are introduced to the model by using the input layer. Hidden layer transfers the received information onto nonlinear future by using an activation function that is selected from a group of functions called basic kernel functions. One of the most popular basic kernel functions that are used in the RBNN method is the Gaussian function. In this function, the largest amount is obtained when the distance between the input vector and the function's centre is equal to zero. Finally, the hidden layer information is cumulated using a linear regressor, and the ultimate result is transferred to the output layer. So that, the jth output is calculated as follow:

$$x_j = f_j(u) = w_{0j} + \sum_{i=1}^L w_{ij} h_i \quad j = 1, 2, \dots, M \quad (2)$$

where w is weight, h is the output of the hidden layer's neurones, L is the number of hidden layer's neurones, and M is the number of outputs that is equal to one in the present study. So that, the final equation of the RBNN model is obtained as follow:

$$x_j = f_i(u) = w_{0j} + \sum_{i=1}^L w_{ij} G(\|u - c_i\|) \quad j = 1, 2, \dots, M \quad (3)$$

where u is the input variable, c_i is the center of the i th kernel, G is the basic kernel function, and $\| \cdot \|$ is the Euclidean distance between u and c_i . The structure of a simple RBNN model is shown in the following Fig. 2.

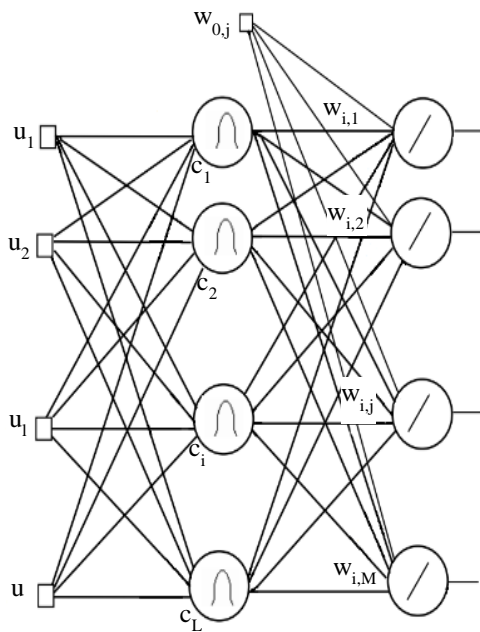


Fig. 2. RBF-NN model structure.

It is obvious that the number of input and output layers' neurones is equal to the number of input and output variables of the considered problem. However, the number of hidden layer's neurones should be determined using the trial and error method.

4. Results and discussion

4.1. Discharge coefficient

The discharge coefficient of a normal weirs is a function of weir crest height (w), total flow head over the weir (h), weir crest thickness, crest shape, vertex configuration, and vertex angle. Also, Kumar et al. (2011) presented a relationship as a function of the vertex angle (θ) and the ratio of the head over weir crest height (h/w) for triangular weir form plan. Therefore, in the present study, the effect of dimensionless parameters, the ratio of the weir crest length to the flow head over weir (L/h), Froude number (F_r), the ratios of head over weir to the channel width (h/B), $\sin \theta \times w/L$ and $w + h/\sin \theta \times w$ on the discharge coefficient of the triangular weir form plan (C_d) are investigated. In the following, with the use of RBNN and M5', six different models are defined as a function of those dimensionless parameters. The combination of input parameters in different models is shown in Fig. 3. To check the accuracy of the RBNN and M5' models results, statistical indices of the mean absolute percent error (MAPE) and correlation coefficients (R^2) are used:

$$MAPE = \frac{1}{n} \sum_{i=1}^n \left| \frac{C_{d(observable)i} - C_{d(predicted)i}}{C_{d(observable)i}} \right| \times 100\% \quad (4)$$

$$R^2 = \frac{(n \sum_{i=1}^n C_{d(predicted)i} C_{d(observable)i} - \sum_{i=1}^n C_{d(predicted)i} \sum_{i=1}^n C_{d(observable)i})^2}{n \sum_{i=1}^n (C_{d(predicted)i})^2 - \sum_{i=1}^n (C_{d(predicted)i})^2 (n \sum_{i=1}^n (C_{d(observable)i})^2 - \sum_{i=1}^n (C_{d(observable)i})^2)} \quad (5)$$

where, $C_{d(Predicted)i}$ and n is the laboratory discharge coefficient, predicted and the number of laboratory measurements, respectively. In this study, 80 % of the data for training and the remained 20 % were used to test the RBNN and M5' models.

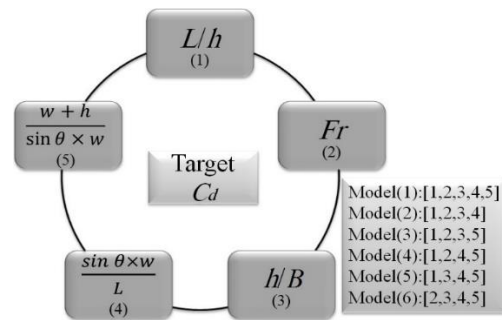


Fig. 3. Combination strategies of input parameters in different models.

4.2. Sensitivity analysis

The result of the sensitivity analysis of the training mode of RBNN method for Models 1 to 6 is shown in Fig. 4. Based on the results of the RBNN method, the MAPE value for Models 1 to 5 is almost predicted similarly. As can be seen from Figure 4a, Model (6) has the lowest error value and the highest correlation coefficients ($R^2 = 0.597, MAPE = 4.816$). Model (6) is a function of the Froude number (F_r), the ratio of the head over the weir to the channel width (h/B) and the ratios $\sin \theta \times w/L$. For the M5' method, the results of the sensitivity analysis of the training mode of models 1 to 6 are shown in Fig. 4b. According to modelling results, Model (4) has the highest error ($MAPE = 3.957$) and the lowest correlation coefficient ($R^2 = 0.740$). In contrast, models 1, 3, and 6 have the least error value and the highest R^2 ($R^2 = 0.844, MAPE = 3.222$). As can be seen, the M5' method predicts the results of models 1, 3 and six quite similar. The mechanism of the M5' method is that calculate the most optimal results for models with lower input parameter numbers and repeated parameters in other models. Therefore, based on the M5' mechanism, Model (1) has five input parameters that L/h , F_r , h/B , $\sin \theta \times w/L$ and $w + h/\sin \theta \times w$ and in models 3 and 6 (models 3 and 6 each have four input parameters) have been repeated. Therefore, the results of all three models 1, 3 and 6 by the M5' method are predicted completely similar. In the following, the results of RBNN and M5' for each of 1 to six are examined.

4.3. Comparison of the results of the RBNN and M5' method in prediction of the weir discharge coefficient

Fig. 5 shows the mean absolute percentage error (MAPE) between RBNN and M5' methods in prediction of the discharge coefficient of triangular weir form plan for models 1 to 6. As can be seen, the value of the Model (1) error for the M5' method in both train and test steps is less than the RBNN method. The MAPE value for the RBNN method in the train and test mode is calculated 7.967 and 6.420, while the M5' method predicts the MAPE value of 3.222 in train mode and 2.774 in the test mode. Similar to Model (2), the error value of the M5' method in both train and test situations is less than the RBNN method. The MAPE for RBNN and M5' methods in train mode is respectively 8.101 and 3.322, and in the test mode, is calculated 5.961 and 3.276, respectively.

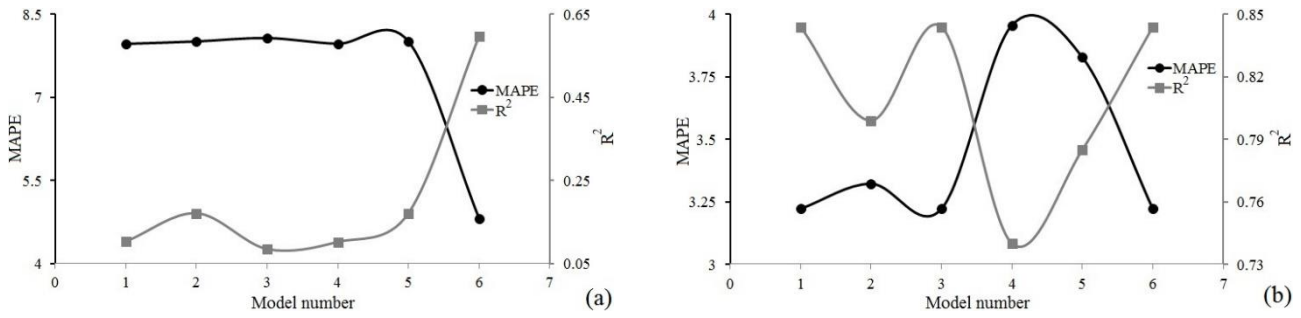
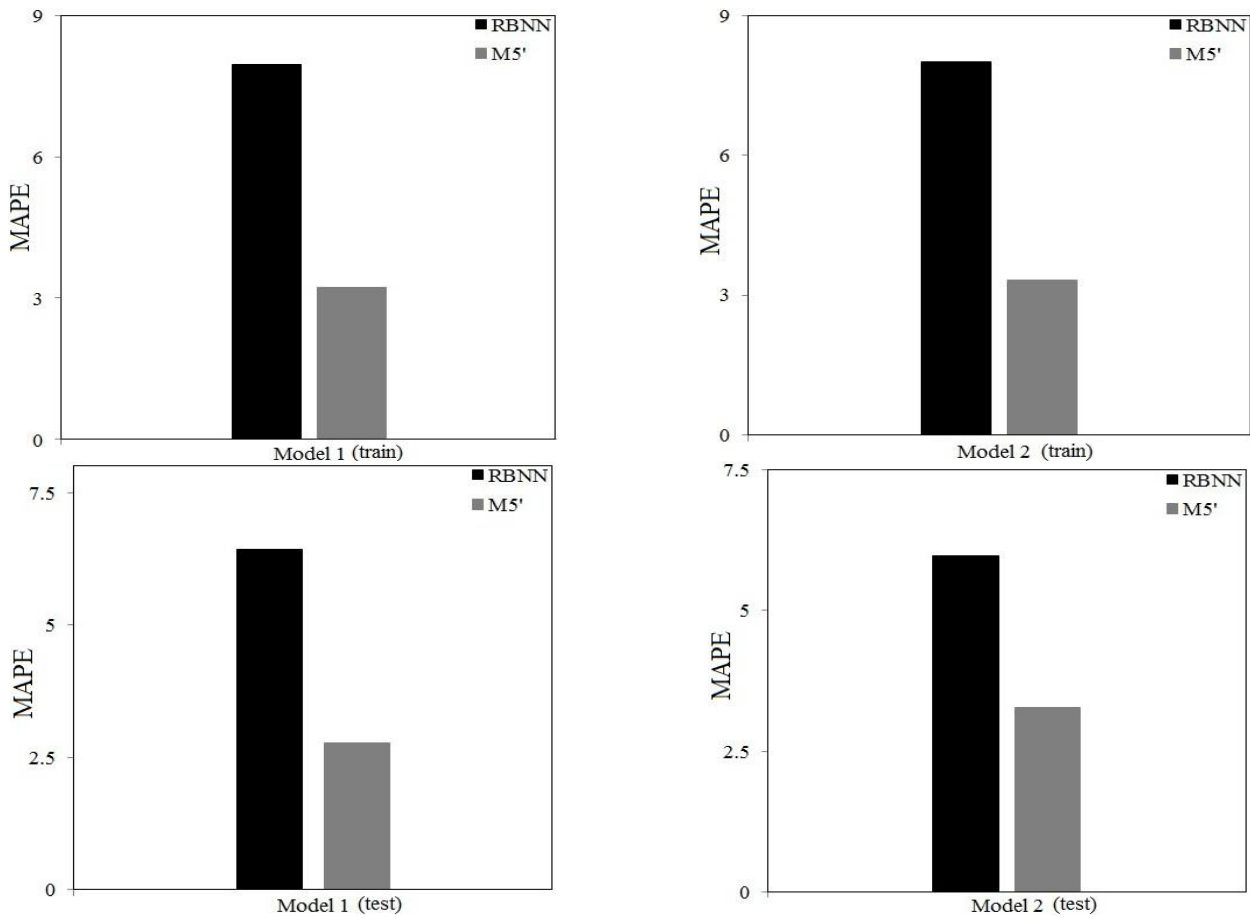


Fig. 4. Comparison of R² and MAPE values for training models 1 to 6 (a) RBNN (b) M5'.

The accuracy of the M5' method to predict the discharge coefficient by Model (3) is higher in the test and train mode than the RBNN method. The mean absolute percentage error calculated in the training mode for the M5' method is 3.222 and for the RBNN method is 8.072. As can be seen, for Model (3), the error of the RBNN method is 2.5 times the M5' method. In train mode, the accuracy of the M5' method is more than the RBNN method. The MAPE in the training mode for the model (4) for M5' and RBNN methods is calculated 3.957 and 7.969, respectively. As shown in Fig. 5, the accuracy of the M5' and RBNN methods in the test mode is approximately the same. In the test mode, the MAPE value for the RBNN method is 6.421 and for the M5' method obtained 6.420. Model (5) is a function of L/h , h/B , $\sin \theta \times w/L$ and

$w + h/\sin \theta \times w$ in both modes the accuracy of the M5' method is more than the RBNN method. The mean absolute percentage error for test and train mode of M5' method is 3.828 and 4.612, respectively, and for the RBNN method is estimated 8.010 and 6.369, respectively. Similar to Models 1 to 5, in both test and train mode, the accuracy of the M5' method is calculated more than the RBNN method. The MAPE values for test and train of the RBNN method was obtained were 4.816 and 5.018, respectively, while MAPE for the M5' method was calculated 3.222 and 2.774 in both test and train modes respectively.



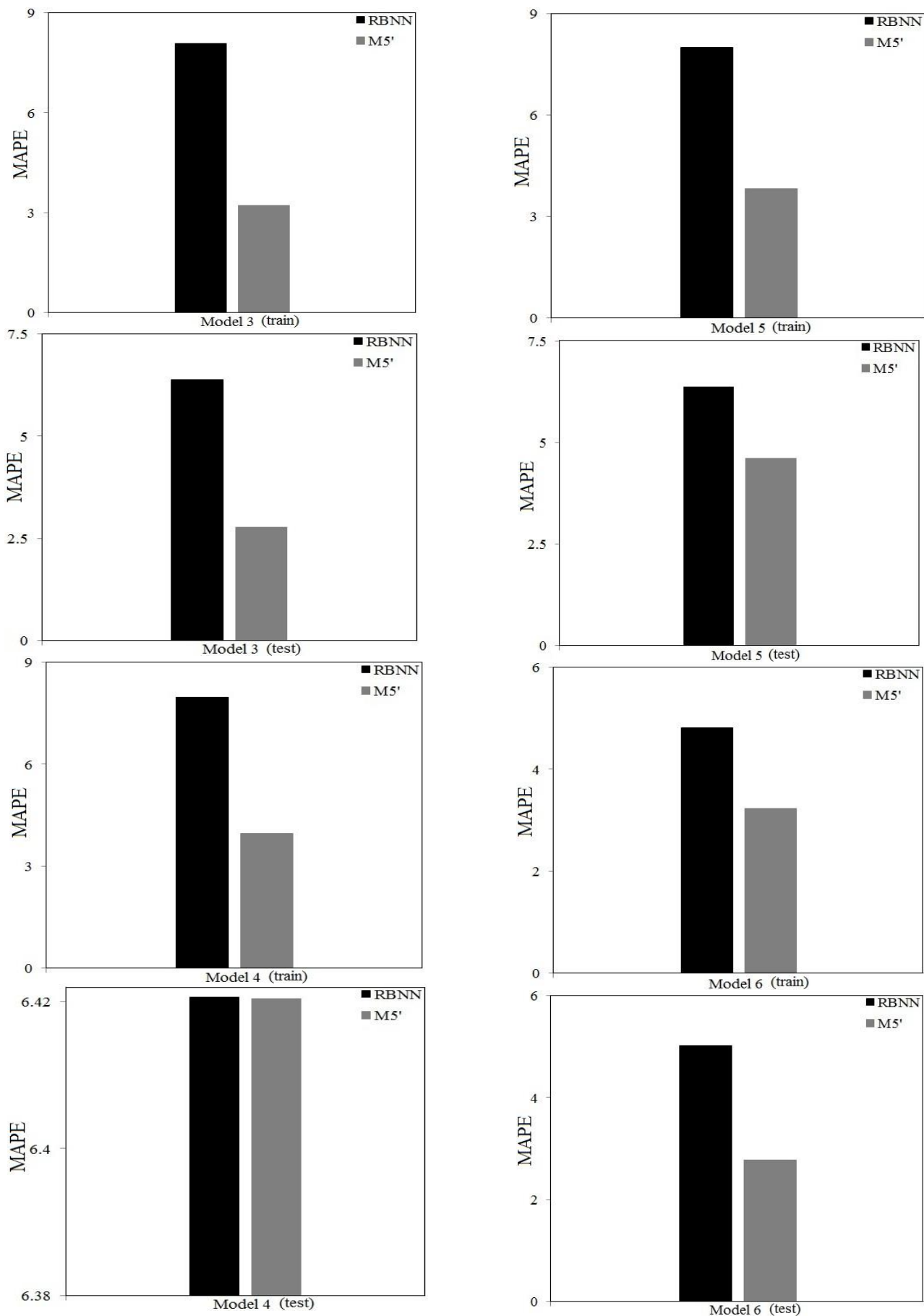


Fig. 5. Comparison of MAPE for different models of RBNN and M5'.

4.4. Derivation of discharge coefficient based on M5'

In Fig. 6, the scatter plots are illustrated for models 1 to 6 of the M5' method. As can be seen, Model (1) is a function of all input parameters. By analyzing the results of Model (1), the following relations are proposed using the M5' method. Based on the results of Model (1), if the values are $h/B \leq 0.08$, the discharge coefficient is a function of h/B . In other words, in this condition, the effect of the parameter h/B is perceptible. Also, if the value is $\sin \theta \times \frac{w}{L} \leq 1.499$, the discharge coefficient is predicted equally to the constant value of 0.739. However, for Froude number less than 0.824 and 0.717, the discharge coefficient is predicted regarding Froude numbers. Therefore, for Model (1) the most important parameters including h/B and Froude numbers. For Model (1):

$$\begin{aligned} &\text{If } h/B \leq 0.08 \\ &C_d = 0.966 - 2.716(h/B) \\ &\text{else} \\ &\text{if } \sin \theta \times \frac{w}{L} \leq 1.499, \\ &C_d = 0.739 \\ &\text{else} \\ &\text{if } (Fr) \leq 0.824 \\ &\text{if } (Fr) \leq 0.717 \\ &C_d = 0.454 + 0.345(Fr) \\ &\text{else} \\ &C_d = 0.898 - 1.034(h/B) \\ &\text{else} \\ &\text{if } (Fr) \leq 1.269 \\ &C_d = 0.615 \\ &\text{else } C_d = 0.666 \end{aligned}$$

Also, by analyzing the modeling results for Model (2), the following relationships are presented. Similar to Model (1), if the value h/B is less than 0.08, the discharge coefficient is predicted only regarding the parameter h/B . For this model, if $(\sin \theta \times w/L) \leq 0.156$ discharge coefficient is a function of the $\sin \theta \times w/L$ Froude number and h/B . In this model, the effects of $w + h/\sin \theta \times w$ being negligible. For Model (2):

$$\begin{aligned} &\text{If } h/B \leq 0.08, C_d = 0.966 - 2.716(h/B) \\ &\text{else} \\ &\text{if } (\sin \theta \times w/L) \leq 0.156 \\ &C_d = 0.671 - 1.149(\sin \theta \times w/L) \\ &\text{else} \\ &C_d = 1.156 - 0.333(Fr) - 1.079(h/B) \end{aligned}$$

The following relationships are presented according to the modeling results. The most effective parameters of this model include h/B , $w + h/\sin \theta \times w$ and Fr . However, the effect of head over the weir to the channel width (h/B) is higher than other parameters. Also, as can be seen, the effect of the parameter L/h on Model (3) is not significant. For Model (3):

$$\begin{aligned} &\text{If } h/B \leq 0.08 \\ &C_d = 0.966 - 2.716(h/B) \\ &\text{else} \\ &\text{if } \sin \theta \times \frac{w}{L} \leq 1.499, \end{aligned}$$

$$\begin{aligned} &C_d = 0.739 \\ &\text{else} \\ &\text{if } (Fr) \leq 0.824 \\ &\text{if } (Fr) \leq 0.717 \\ &C_d = 0.454 + 0.354(Fr) \\ &\text{else} \\ &C_d = 0.898 - 1.034(h/B) \\ &\text{else} \\ &\text{if } (Fr) \leq 1.269 \\ &C_d = 0.615 \\ &\text{else} \\ &C_d = 0.666 \end{aligned}$$

The proposed relationship for Model (4) is presented below. In this model, if the value L/h is less than 12,682 and $\sin \theta \times w/L$ smaller than 0.171, the triangular weir discharge coefficient is a function of the parameter L/h and the Froude number. In other words, in Model (4) the effect of parameters $\sin \theta \times w/L$ and $w + h/\sin \theta \times w$ is insignificant in the modeling of the discharge coefficient. For Model (4):

$$\begin{aligned} &\text{If } L/h \leq 12.682 \\ &\text{if } (\sin \theta \times w/L) \leq 0.171 \\ &C_d = 0.707 - 0.008(L/h) \\ &\text{else} \\ &C_d = 0.947 - 0.025(L/h) - 0.533(Fr) \\ &\text{else} \\ &C_d = 0.813 - 0.004(L/h) - 0.122(Fr) \end{aligned}$$

For Model (5) the effect of the Froude number has been removed. For this model, if h/B is smaller than 0.08, the discharge coefficient is a function of the h/B . However, for $w + h/\sin \theta \times w$ less than 1.499, the value of the discharge coefficient is equal to the constant value of 0.739. Also, for a $w + h/\sin \theta \times w$ lower than 1.809, the discharge coefficient is predicted based on h/B . In general, in this model, the effect of the parameter h/B is significant, and in contrast, the impact of $\sin \theta \times w/L$ and v is negligible. For Model (5):

$$\begin{aligned} &\text{If } h/B \leq 0.08 \\ &C_d = 0.966 - 2.716(h/B) \\ &\text{else} \\ &\text{if } (w + h/\sin \theta \times w) \leq 1.499 \\ &C_d = 0.739 \\ &\text{else} \\ &\text{if } (w + h/\sin \theta \times w) \leq 1.809 \\ &C_d = 0.840 - 1.112(h/B) \\ &\text{else} \\ &\text{if } (\sin \theta \times w/L) \leq 0.114 \\ &C_d = 0.669 \\ &\text{else} \\ &C_d = 0.711 \end{aligned}$$

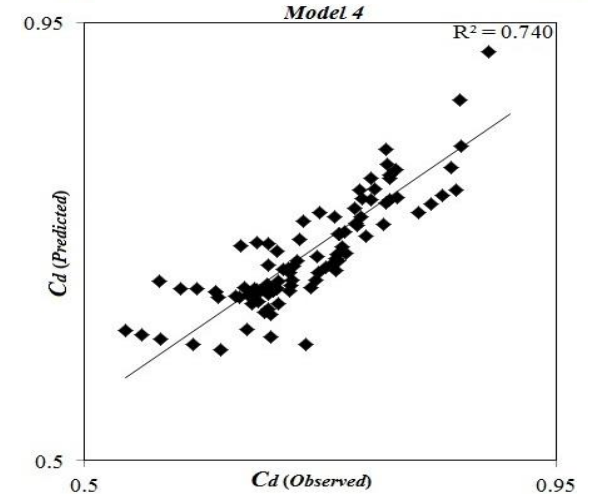
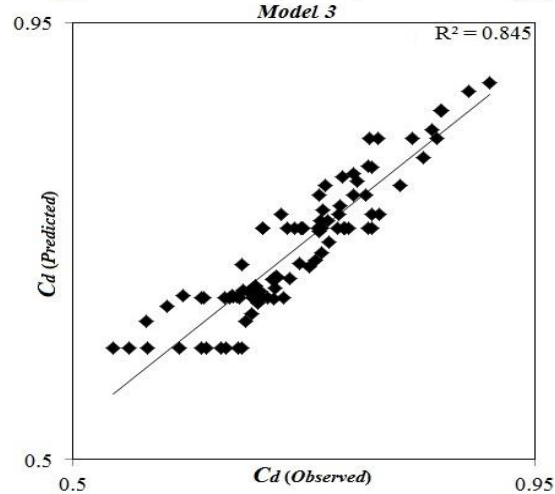
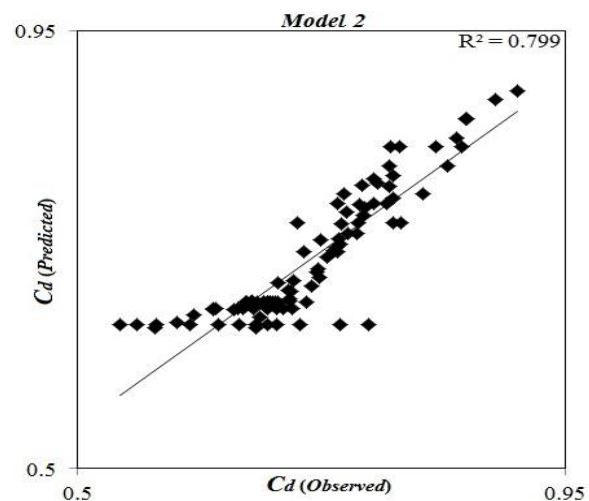
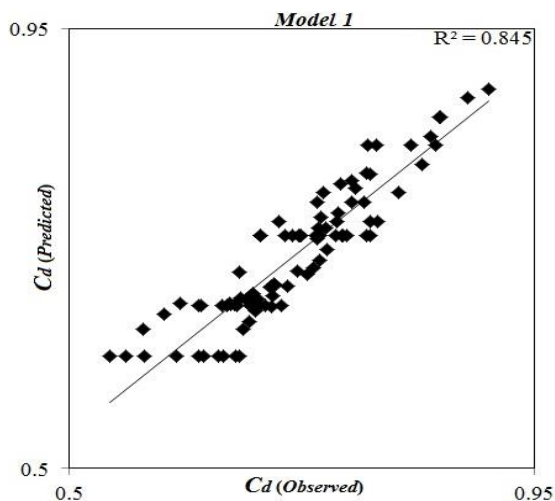
For Model (6) the effect of the parameter L/h is ignored. In this model, the effect of the parameters h/B and Fr is greater than the other input parameters. For example, for h/B values less than 0.08, the triangular weir discharge is considered by parameter h/B . Also, if the $w+h/\sin\theta \times w$ value is less than 1.499, the value of the discharge coefficient is equal to the constant value of 0.739. As can be seen, for Model (1) to Model (6) the parameters h/B and Fr are introduced as the most effective parameters. For Model (6):

$$\begin{aligned} &\text{if } h/B \leq 0.08 \\ &C_d = 0.966 - 2.716(h/B) \\ &\text{else} \\ &\text{if } (w+h/\sin\theta \times w) \leq 1.499 \\ &C_d = 0.739 \\ &\text{else} \\ &\text{if } (Fr) \leq 0.824 \\ &\text{if } (Fr) \leq 0.717 \\ &C_d = 0.454 + 0.354(Fr) \\ &\text{else} \\ &C_d = 0.898 - 1.034(h/B) \\ &\text{else} \end{aligned}$$

$$\begin{aligned} &\text{if } (Fr) \leq 1.269 \\ &C_d = 0.615 \\ &\text{else} \\ &C_d = 0.666 \end{aligned}$$

5. Conclusions

Normal weir is installed in open channels as a simple plane to adjust and measure the flow. As the flow approaches the normal weir location, the flow from the weir crest to the downstream channel is thrown. Normal weirs are divided into two types: sharp-crested and broad-crested weirs. The sharp-crested weirs as rectangular, triangular, circular, Sutro and triangular plan form weirs are used. In this study, the triangular plan form weirs model was modeled using Radial Base Neural Networks (RBNN) and Method modified 5 (M5') methods. For this purpose, effective parameters were first identified on the discharge coefficient. Then, by combining the input parameters, for each of the RBNN and M5' methods, six different models were introduced. By comparing the results of six defined models, the M5' model is more accurate. The superior model was also introduced with sensitivity analysis. The superior model, model the discharge coefficient regarding all input parameters. In the following, for each M5' model, relationships were proposed to predict the discharge coefficient. The analysis of these relationships showed that the parameters of head over the weir to the channel width and Froude number are the most effective parameters in the prediction of the triangular plan form weirs.



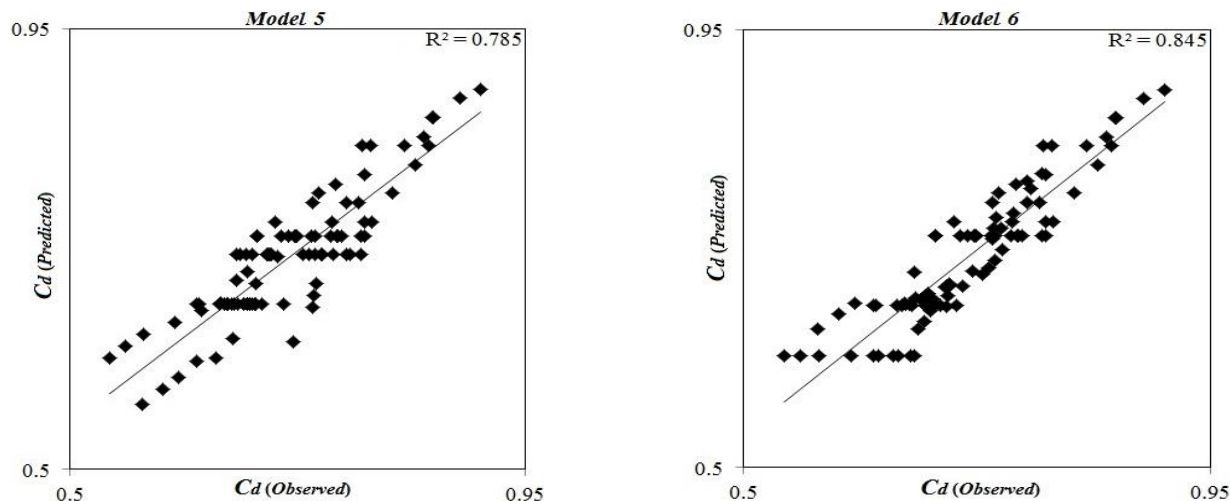


Fig. 6. Results of the predicted discharge coefficient by the M5 method for models 1 to 6.

References

- Ay M., Kisi O., Modeling of dissolved oxygen concentration using different neural network techniques in Foundation Creek, El Paso County, Colorado, *Journal of Environmental Engineering* 138 (2011) 654-662.
- Azamathulla H.M., Ahmad Z., computation of discharge through side sluice gate using gene-expression programming, *Irrigation and Drainage* 62 (2013) 115-119.
- Bagheri S., Heidarpour M., Flow over rectangular sharp-crested weirs, *Irrigation science* 28 (2010) 173.
- Bilhan O., Emiroglu M.E., Kisi O., Application of two different neural network techniques to lateral outflow over rectangular side weirs located on a straight channel, *Advances in Engineering Software* 41 (2010) 831-837.
- Breiman L., Friedman J., Stone C.J., Olshen R.A., *Classification and regression trees*, CRC press (1984).
- Broomhead D.S., Lowe D., Radial basis functions, multi-variable functional interpolation and adaptive networks, *Royal Signals and Radar Establishment Malvern (United Kingdom)* (1988).
- Dursun O.F., Kaya N., Firat M., Estimating discharge coefficient of semi-elliptical side weir using ANFIS, *Journal of hydrology* 426 (2012) 55-62.
- Ebtehaj I., Bonakdari H., Khoshbin F., Azimi H., Pareto genetic design of group method of data handling type neural network for prediction discharge coefficient in rectangular side orifices, *Flow Measurement and Instrumentation* 41 (2015) 67-74.
- Emiroglu M.E., Baylar A., Closure to Influence of Included Angle and Sill Slope on Air Entrainment of Triangular Planform Labyrinth Weirs, *Journal of Hydraulic Engineering* 132 (2006) 748-748.
- Giustolisi O., Using genetic programming to determine Chezy resistance coefficient in corrugated channels, *Journal of Hydroinformatics* 6 (2004) 157-173.
- Hager W.H., *Hydraulics of plane free overfall*, *Journal of Hydraulic Engineering* 109 (1983) 1683-1697.
- Hand D.J., *Principles of data mining*, *Drug safety* 30 (2007) 621-622.
- Hay N., Taylor G., A computer model for the determination of the performance of labyrinth weirs. 13th Congress of IAHR, Koyoto, Japan (1969).
- Johnson M.C., Discharge coefficient analysis for flat-topped and sharp-crested weirs, *Irrigation science* 19 (2000) 133-137.
- Kandaswamy P., Rouse H., Characteristics of flow over terminal weirs and sills, *Journal of the Hydraulics Division* 83 (1957) 1-13.
- Kantardzic M., *Data mining: concepts, models, methods, and algorithms*, John Wiley & Sons (2011).
- Kisi O., Emiroglu M. E., Bilhan O., Guven A., Prediction of lateral outflow over triangular labyrinth side weirs under subcritical conditions using soft computing approaches, *Expert systems with Applications* 39 (2012) 3454-3460.
- Kisi O., Yuksel I., Dogan E., Modelling daily suspended sediment of rivers in Turkey using several data-driven techniques/Modélisation de la charge journalière en matières en suspension dans des rivières turques à l'aide de plusieurs techniques empiriques *Hydrological Sciences Journal* 53 (2008) 1270-1285.
- Kumar S., Ahmad Z., Mansoor T., A new approach to improve the discharging capacity of sharp-crested triangular plan form weirs, *Flow Measurement and Instrumentation* 22 (2011) 175-180.
- Moody J., Darken C.J., Fast learning in networks of locally-tuned processing units, *Neural computation* 1 (1989) 281-294.
- Poggio T., Girosi T., Regularization algorithms for learning that are equivalent to multilayer networks, *Science (Washington)* 247 (1990) 978-982.
- Quinlan J.R., *Learning with continuous classes*. 5th Australian joint conference on artificial intelligence, Singapore (1992).
- Ramamurthy A.S., Tim U.S., Rao M., Flow over sharp-crested plate weirs, *Journal of irrigation and drainage Engineering* 113 (1987) 163-172.
- Rouse H., Discharge characteristics of the free overfall: Use of crest section as a control provides easy means of measuring discharge, *Civil Engineering* 6 (1936) 257-260.
- Savic D.A., Walters G.A., Davidson J.W., A genetic programming approach to rainfall-runoff modelling, *Water Resources Management* 13 (1999) 219-231.
- Schoder E.W., Turner K.B., Precise weir measurements, *Transactions of the American Society of Civil Engineers* 93 (1929) 999-1110.

- Strelkoff T.S., Solution of Highly Curvilinear Gravity Flow, Journal of the Engineering Mechanics Division 90 (1964) 195-222.
- Swamee P.K., Generalized rectangular weir equations, Journal of Hydraulic Engineering 114 (1988) 945-949.
- Taylor G., The performance of labyrinth weirs, University of Nottingham (1968).
- Tullis B.P., Young J., Chandler M., Head-discharge relationships for submerged labyrinth weirs, Journal of Hydraulic Engineering 133 (2007) 248-254.
- Tullis J.P., Amanian N., and Waldron D., Design of labyrinth spillways, Journal of hydraulic engineering 121 (1995) 247-255.
- Wang Y., Witten I.H., Induction of model trees for predicting continuous classes (1996).
- Wormleaton P.R., Soufiani E., Aeration performance of triangular planform labyrinth weirs, Journal of environmental engineering 124 (1998) 709-719.